BNL-205717-2018-BOOK

A (Sub)Micro-Scale Investigation of Fe Plaque Distribution in Selected Wetland Plant Root Epidermis

H. Feng,

To be published in "Trace Metals: Evolution, Environmental and Ecological Significance"

September 2017

Computational Science Initiative

Brookhaven National Laboratory

U.S. Department of Energy

USDOE Office of Science (SC), Advanced Scientific Computing Research (SC-21)

DISCLAIMER

(SUB)MICRO-SCALE INVESTIGATION OF FE PLAQUE DISTRIBUTION IN SELECTED WETLAND PLANT ROOT EPIDERMIS

Huan Feng[1*], Weiguo Zhang[2], Jia-Jun Wang[3] , Yu Qian[4], Frank J. Gallagher[5], Lizhong Yu[2], Wenliang Liu[2], Houjun Liu[6], Yuanyi Li[1, 7], Manoj D. Mahajan[8], Jun Wang[3], Christopher Eng[3], Keith W. Jones[9], Chang-Jun Liu[10], Ryan Tappero[3]

1. Department of Earth and Environmental Studies, Montclair State University, Montclair, New Jersey 07043, USA
2. State Key Laboratory of Estuarine and Coastal Research, East China Normal University, Shanghai 200062, PRC
3. Photon Sciences Directorate, Brookhaven National Laboratory, Upton, New York 11973, USA
4. School of Ecology and Environmental Sciences, Yunnan University, Kunming, Yunnan 650091, PRC
5. Urban Forestry Program, Department of Ecology, Evolution and Natural Resources, Rutgers, The State University of New Jersey, New Brunswick, New Jersey 08901, USA
6. College of Land and Environment, Shenyang Agricultural University, Shenyang 110866, PRC
7. Department of Mechanics, School of Mechanical Engineering, Tianjin University, Tianjin 300072, PRC
8. Department of Technology and Society, Stony Brook University, Stony Brook, New York 11794, USA

9. Environmental Sciences Department, Brookhaven National Laboratory, Upton, New York 11973, USA
10. Biological Sciences Department, Brookhaven National Laboratory, Upton, New York 11973, USA

*Corresponding author: fengh@mail.montclair.edu (H. Feng)

ABSTRACT

This study focuses on investigation of the distribution of Fe plaque in the root epidermis of the selected wetland plant species (*Phragmites australis, Typha latifolia* and *Spartina alterniflora*) using synchrotron X-ray microfluoresces, X-ray absorption near edge structure and transmission X-ray microscope techniques with (sub)micro-scale resolution. The wetland plants were collected in Liberty State Park, New Jersey, USA, and Yangtze River intertidal zone, Shanghai, China, respectively, during the different time period. Although a number of early studies have reported that Fe-oxides can precipitate on the surface of aquatic plants in the rhizosphere to form iron plaque, the role of Fe plaque in regulating metal biogeochemical cycle has been in discussion for decades. The results from this study show that Fe is mainly distributed in the epidermis non-uniformly, and the major Fe species is ferric Fe (Fe^{3+}). This information is needed to make broad inferences about the relevant plant metal uptake mechanisms because Fe accumulation and distribution in the root system is important to understanding the metal transport processes that control the mobility of metals in plants. This study improves our

understanding of Fe plaque distributions and speciation in the wetland plant root system, and helps us to understand the function of Fe plaque in metal transport and accumulation through the root system.

Keywords: Wetland plant; Root epidermis; Iron plaque; Synchrotron X-ray radiation technique; Rhizosphere

1. INTRODUCTION

Many studies have shown that wetland plants can uptake Fe and other metals from rhizosphere soils and sediments through the root system and store these metals within the plant biomass [1-6]. Iron (Fe) plaque was found on the root surface of aquatic and terrestrial plant roots [3-5, 7-11]. It was reported that the main species of iron plaque comprises of mainly ferric hydroxides, goethite, and lepidocrocite and minor siderite, whose structure is characterized as amorphous or crystalline iron (oxyhydr) oxides [3, 12]. Due to adsorption or co-precipitation mechanisms, Fe plaque can sequester metals, metalloids and anions in plant roots [12-14]. Some studies indicate that the formation of Fe plaque on root surface of aquatic plants may provide a means of attenuation and external exclusion of metals [15, 16]. This suggests that Fe plaque may serve as a barrier preventing heavy metals from entering plant roots [7, 17, 18]. However, Ye et al. (1998) investigated the effects of Fe plaque on the growth of *Typha latifolia* and reported that the presence of Fe plaque on the root surface did not alter Zn, Pb, and Cd translocation in seedlings in the nutrient solutions. Therefore, the study suggests that Fe plaque is not the main barrier [19]. Regardless if the Fe plaque that formed on the root surface can act as a barrier to prevent metals

from entering the vascular bundle by scavenging these metals, significant correlations between metals and Fe have been found in several studies [11, 18, 20-26]. Nevertheless, high-resolution information of Fe plaque spatial distribution in the plant root systems is still lacking.

In order to understand the function of Fe plaque inside the root system, more detailed information on accumulation and distribution of Fe plaque in the root system should be further explored with the advancement of analytical technology and techniques. Moreover, investigation of the Fe plaque requires high-sensitivity and high resolution analytical apparatus and techniques, such as the high resolution synchrotron X-ray microscope. These techniques have important applications in studying metal translocation and accumulation in plants with (sub)micrometer scale resolution [22-25, 27, 28]. Unlike the conventional wet chemistry analyses, the high resolution synchrotron X-ray measurement of Fe plaque distributions in plant roots can lead to a better understanding of Fe transport and fate in the plants. In this study, synchrotron X-ray microfluoresces (μXRF), synchrotron X-ray absorption near edge structure (XANES) and synchrotron transmission X-ray microscope (TXM) techniques are applied to this investigation. The purpose of this study is to examine spatial distribution of Fe plaque in the root epidermis of selected wetland plants.

2. MATERIALS AND METHODS

2.1 *Sample collection and preparation*

Wetland plant samples were collected in Liberty State Park, New Jersey, USA, and the Yangtze River intertidal zone, Shanghai, China, respectively (Figure 1). The field work for collection of *Typha latifolia* and *Phragmites australis* at Liberty State Park, a brownfield site in northern New Jersey (Figure 1a), was conducted between 2010 and 2014. The field work in the Yangtze River estuary, one of the largest estuaries in the world, was conducted in 2006 and 2013, respectively. *Phragmites australis* and *Spartina alterniflora*, two abundant local wetland plant species, were sampled in Chongming Island in the Yangtze River intertidal zone (Figure 1b). All of the samples collected in Liberty State Park were collected along with soils using stainless steel spades and placed into large plastic containers and then transported to Montclair State University. Similarly, all of the samples collected in the Yangtze River intertidal zone were also collected along with soils using stainless steel spades and placed into large plastic containers and then transported to East China Normal University. Further sample treatments were conducted at Montclair State University and East China Normal University, respectively. The bulk soils were easily removed from the plants by gentle shaking by hand. The trace residual soils on the roots were rinsed off with small amounts (<20 ml) of deionized water. Some of the root samples were freshly processed for immediate synchrotron radiation measurement. The thin root cross-sections for synchrotron X-ray microfluorescence (μXRF) measurement were made at -20°C in the compartment of a cryotome (Cryostat CM1950, Leica Microsystems) by suspending the root sample in an optimal cutting temperature (OCT) compound (Surgipath Medical Industries, Surgipath, Canada) that does not infiltrate the specimen. Once the OCT solidified, the cryotome was used to cut a 20–50 μm thin section of the root samples. The thin sections were then mounted on a 25 mm × 76 mm quartz microscope slide (SPI Supplies®) for synchrotron μXRF analysis. For synchrotron transmission X-ray microscope (TXM)

measurement and synchrotron X-ray absorption near edge structure (XANES) measurement to investigate Fe plaque, each of the root samples was glued on the tip of a needle and then mounted on a stand. All the samples prepared for synchrotron X-ray measurement were kept in our low temperature laboratory (4ºC) or in a desiccator at the beamline work station before the analysis.

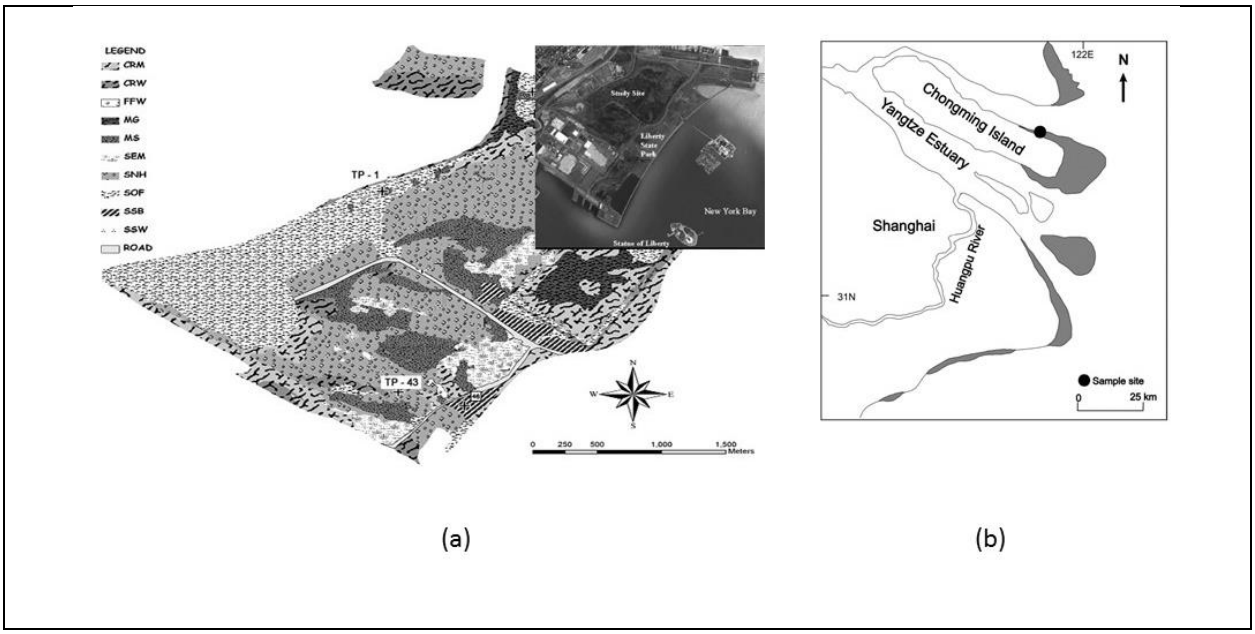

Figure 1 Map showing the study areas in (a) Liberty State Park, New Jersey, USA, and (b) Yangtze River intertidal Zone, China.

2.2 *Synchrotron X-ray fluorescence measurement*

Synchrotron X-ray microfluorescence (μXRF) images were acquired from National Synchrotron Light Source (NSLS) X27A Beamline at Brookhaven National Laboratory (Upton, NY)[29]. Briefly, this bend-magnet beamline uses Kirkpatrick-Baez (K-B) mirrors to produce a focused spot (10 μm × 10 μm or 15 μm × 15 μm) of hard X-rays with tunable energy achieved via Si(111) or Si(311) channel-cut monochromator crystals. In the synchrotron μXRF

measurement, the incident beam energy was fixed at 13.5 keV to excite all target elements simultaneously. The sample was oriented 45° to the incident beam, and rastered in the path of the beam by an XY stage while X-ray fluorescence was detected by a 13-element Canberra Ge array detector positioned 90° to the incident beam. Elemental maps for root cross-section were typically collected from a 1 mm^2 sample area using a step size of 10 μm or 20 μm and a dwell time of 7 seconds. The fluorescence yields were normalized to the changes in intensity of the X-ray beam (I_0) and the dwell time. During the measurement, the X-ray influences were comparatively low and radiation damage effects were minimal. Data acquisition and processing were initially performed using IDL-based software at X27A Beamline. Further data analysis was conducted at Montclair State University.

2.3 *Synchrotron transmission X-ray microscope and X-ray absorption near edge microstructure measurement*

Synchrotron transmission X-ray microscope analysis was conducted at National Synchrotron Light Source (NSLS) X8C Beamline at Brookhaven National Laboratory (Upton, NY) and Advanced Photon Source (APS) 8BM Beamline at Argonne National Laboratory (Argonne, IL) that were equipped with a full-field transmission X-ray microscope (TXM) manufactured by Xradia, Inc [30]. The newly developed TXM provides a large field of view (40 μm× 40 μm), 30 nm resolution, local tomography, and automated maker-free image acquisition and alignment [30]. By tuning X-ray energy across the absorption edge of the element of interesting, this TXM technique enables chemical information with high sensitivity [31, 32]. In order to identify Fe plaque in the roots, synchrotron X-ray absorption near edge structure

(XANES) measurement were performed on the samples in this study. The energy was set both below and above Fe K-edge (7112 eV) by scanning the X-ray energy from 7092 eV to 7192 eV passing through Fe K-edge with a step size of 2 eV. A stack of images was thus obtained. A lens-coupled scintillator with a 2048 × 2048 pixel camera detector was used to record the images. A full spectrum for each pixel was extracted for all 1024 × 1024 pixels with 2×2 binning. All the XANES analysis was carried out using Matlab (MathWorks) and a customized program developed in house (former Beamline X8C group, NSLS, BNL). Background normalization was made first for the TXM images with a background image collected at every energy. Synchrotron XANES fitting was performed with the classic linear combination fitting method as described in our previous work [31, 33]. Synchrotron X-ray absorption near edge microstructure (μXANES) spectroscopy was further applied to determine Fe oxidation state of the Fe plaque in the root epidermis. The standard reference materials, which contain Fe (Fe^0), α-Fe_2O_3 (Fe^{3+}) and Fe_3O_4 (Fe^{3+} and Fe^{2+} mixture) (Sigma, USA), were used in the measurement. The standard XANES spectra were collected under the same condition as the root sample XANES measurement and the pre-edges of Fe^0, Fe^{2+}, and Fe^{3+} in the standard reference materials were recorded during the measurement. According to the defined pre-edge of Fe^0, α-Fe_2O_3 and Fe_3O_4, in the standard reference materials, the Fe pre-edges of the samples were fitted to the Fe pre-edge of the standard reference materials to determine the Fe speciation of Fe plaque in the samples.

3. RESULTS AND DISCUSSION

Accumulation of Fe plaque in the root epidermis can be a complex biogeochemical process. Figures 2 and 3 show synchrotron μXRF measurement of Fe concentrations and

distributions in the root samples of *Typha latifolia*, *Phragmites australis* and *Spartina alterniflora*. Cross-section measurement on *Phragmites australis* (Figure 2c and 2d) and *Spartina alterniflora* (Figure 3d) show apparently difference in Fe concentration between the epidermis and the vascular bundle. Relatively high Fe concentration was found in the epidermis of these root samples with a patchy distribution pattern. The results indicate that Fe is not uniformly accumulated in the root tissue and transported from the epidermis to the vascular bundle without a concentration gradient. Iron (Fe) is concentrated on the exterior of the root forming a nearly continuous rind on the root epidermis with high Fe concentrations in several discrete zones (Figures 2 and 3). Heterogeneous accumulation of Fe forming a surficial rind found in this study is also consistent with that in other studies [16, 23-25, 34, 35]. [5]. Due to formation of Fe plaque on or near the root surface, Fe shows a relatively high concentration in epidermis.

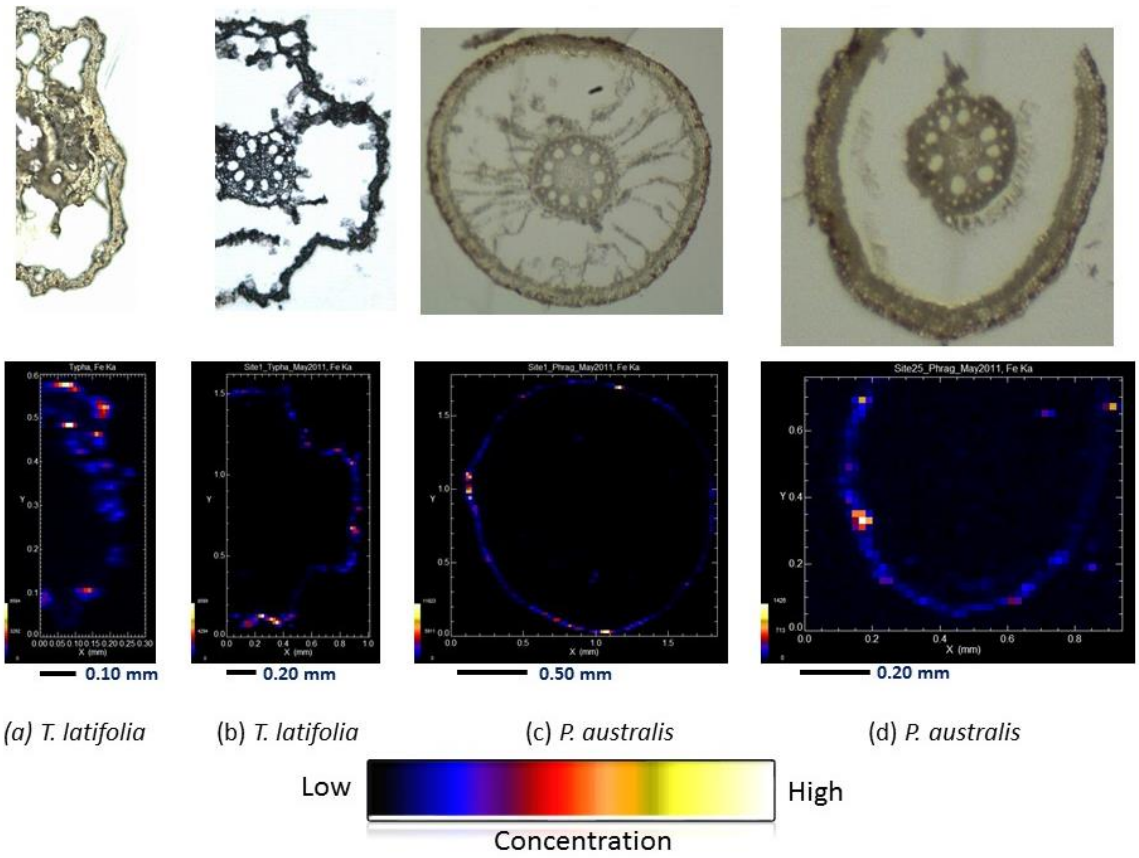

Figure 2. Optical microscopic images of the wetland plant root samples (upper panel) and synchrotron X-ray fluoresce measurement of Fe distributions in the root tissues (lower panel). These samples were collected in Liberty State Park, New Jersey. The species of these samples are identified as follows: (a) *Typha latifolia* root samples collected at Site 1 in June 2010; (b) *Typha latifolia* root sample collected at Site 1 in May 2011; (c) *Phragmites australis* root sample collected at Site 1 in May 2011; and (d) *Phragmites australis* root sample collected at Site 25 in May 2011. For the synchrotron XRF images in the lower panel, higher fluorescence intensity (corresponding to higher concentrations) are nearer to pale yellow and lower intensities are nearer to dark blue according to the color bars. The root thin section is 30 μm in thickness. The resolution is 20 μm per pixel.

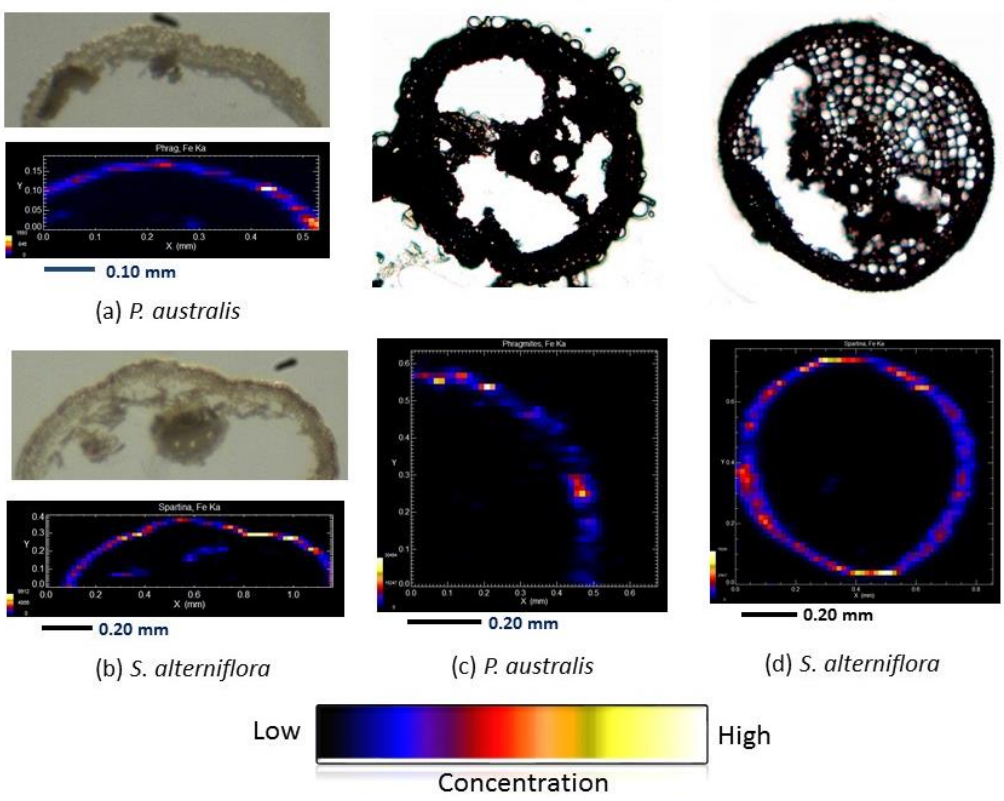

Figure 3. Optical microscopic images of the wetland plant root samples (upper panel) and synchrotron X-ray fluoresce measurement of Fe distributions in the root tissues (lower panel). These samples were collected in collected in Yangtze River intertidal zone, Chongming Island, Shanghai. The species of these samples are identified as follows: (a) *Phragmites australis* root sample collected in October 2006; (b) *Spartina alterniflora* root sample collected in October 2006; (c) *Phragmites australis* root sample collected at Site 2-1 in July 2013; and (d) *Spartina alterniflora* root sample collected at Site 4-2 in July 2013. For the synchrotron XRF images in the lower panel, higher fluorescence intensity (corresponding to higher concentrations) are nearer to pale yellow and lower intensities are nearer to dark blue according to the color bars. The thickness of the cross sections is 50 μm. The resolution is 15 μm per pixel.

The presence of Fe plaque on plant root surface may affect metal uptake. Because of its high adsorption capacity, Fe plaque can sequester other metals and metalloids by adsorption or co-precipitation, causing interferences with the availability of these elements in the rhizosphere and their uptake by and translocation in plants. Therefore, the root epidermis is an important reservoir for deposition of Fe nanoparticles or Fe plaque although Fe oxide species may vary in their formation mechanisms, transport pathways, and reactivity towards other metals, such as Cd, Cu, Co, Cr, Mn, Ni, Pb, and Zn. Previous studies have found that metals in the wetland plants (e.g., *Phragmites australis, Typha latifolia* and *Spartina alterniflora)* have shown significant correlations ($p < 0.001$) with Fe in the plant roots, suggesting a close association of these metals with Fe plaque [23-25].

As shown in Figures 4 and 5, synchrotron TXM measurement on the root samples indicate the presence of Fe plaque in most of these measurement. Since the Fe-based phases can only be observed at the energy above Fe K-edge (7112 keV), a comparison of the paired images of each sample unambiguously confirms whether or not the presence of Fe plaque exists in the sample (Figures 4 and 5). For example, among the samples collected in Liberty State Park Fe was found in the sample shown in Figure 4 (d) by comparison of both images measured above and below the Fe edge. This is *Phragmites australis* root sample collected at Site 25 in May 2011. However, there seems no Fe found in the given sample shown in Figures 4(a), 4(b) and 4(c), which are *Typha latifolia* root sample collected at Site 1 in June 2010, *Typha latifolia* root sample collected at Site 1 in May 2011, and *Phragmites australis* root sample collected at Site 1 in May 2011, respectively. In addition, among the samples collected in the Yangtze River intertidal zone, Fe was found in *Phragmites australis* root samples collected in October 2006 and

July 2013, respectively, as shown in Figures 5 (a) and 5(c) by comparison of both images above and below the Fe edge. However, there seemed no Fe found in the given *Spartina alterniflora* root samples collected in October 2006 and July 2013, respectively, as shown in Figures 5(b) and 5(d). It should be pointed out that, although Fe plaque was not observed in some of these measurement, it does not mean that there is no Fe plaque present in those root samples.

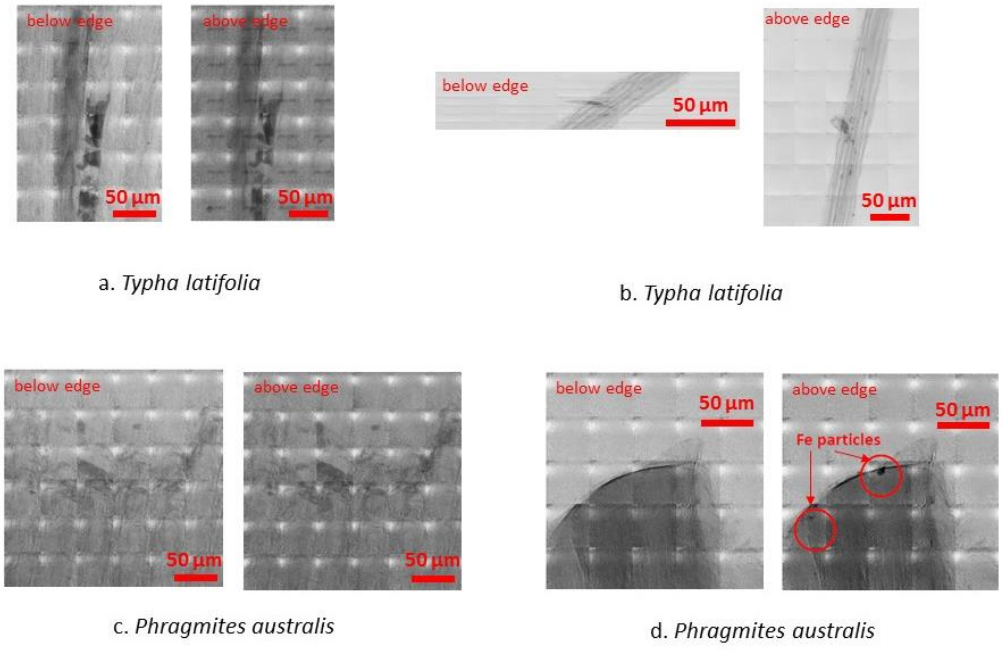

Figure 4. Synchrotron TXM XANES investigation of Fe plaque distributions in the root epidermis. These samples were collected in Liberty State Park, New Jersey. The species are identified as follows: (a) *Typha latifolia* root samples collected at Site 1 in June 2010; (b) *Typha latifolia* root sample collected at Site 1 in May 2011; (c) *Phragmites australis* root sample collected at Site 1 in May 2011; and (d) *Phragmites australis* root sample collected at Site 25 in May 2011. Between the paired images in each set, the image on the left side was measured below the Fe edge, and the one on the right side was measured above the Fe edge. The dark area in the red circle measured above the Fe edge suggests the presence of Fe plaque. The resolution is 30-nm per pixel.

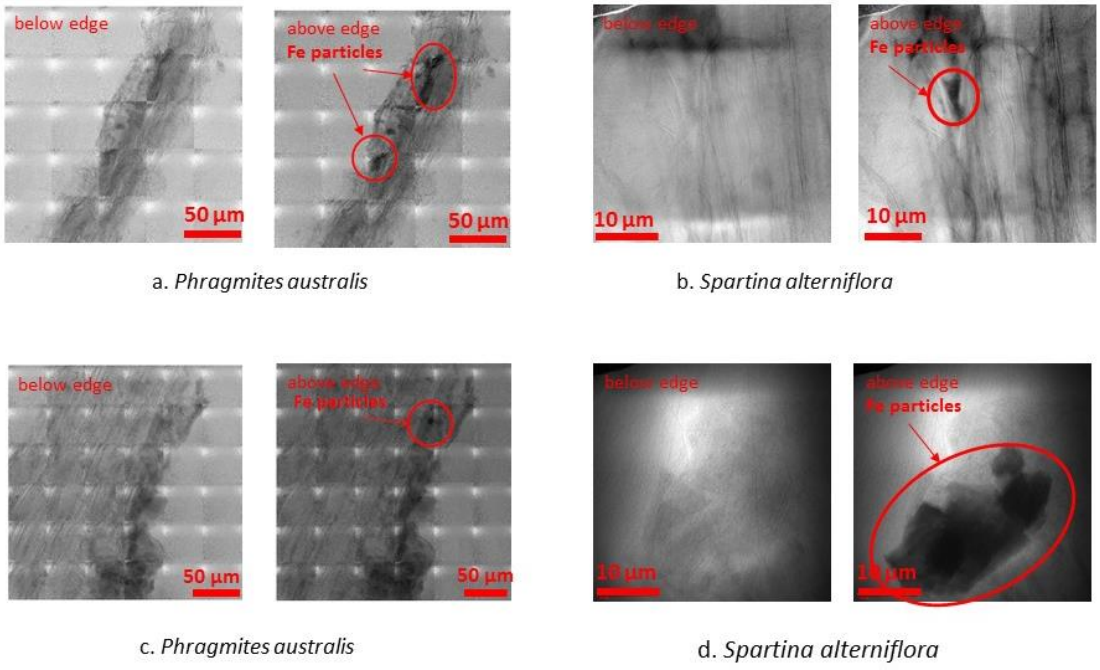

Figure 5. Synchrotron TXM XANES investigation of Fe plaque distributions in the root epidermis. These samples were collected in collected in Yangtze River intertidal zone, Chongming Island, Shanghai. The species are identified as follows: (a) *Phragmites australis* root collected in October 2006; (b) *Spartina alterniflora* root sample (Sample #4) collected in October 2006; (c) *Phragmites australis* root collected at Site 2-1in July 2013; and (d) *Spartina alterniflora* root sample collected at Site 4-2 in July 2013. Between the paired images in each set, the image on the left side was measured below the Fe edge, and the one on the right side was measured above the Fe edge. The dark area in the red circle measured above the Fe edge suggests the presence of Fe plaque. The resolution is 30-nm per pixel.

Root radial oxygen loss (ROL) rates are considered as the key biotic factor controlling Fe plaque formation although ROL is not within the topic of this study. The oxygenation of plant roots by radial oxygen loss (ROL) converts Fe^{2+} to Fe^{3+} and results in the formation of Fe-plaque around roots [6, 36-41]. As shown in Figures 4 and 5, the biochemical complexity and heterogeneity within the rhizosphere may explain unevenly accumulation of Fe on the root epidermis, and the formation of Fe oxide or hydroxide. In this study, Fe speciation in the root epidermis was examined. The results indicate that Fe^{3+} is the predominant species of Fe plaque (Figure 6). There is no other Fe species (i.e., Fe^0 and Fe^{2+}) found in the Fe plaque during the measurement as shown in Figure 6, although specific Fe-containing mineral phase are not identified in this study. However, metal biogeochemical cycling by forming less mobile metal-mineral species with Fe has been reported in previous studies [7, 22, 34, 42]. In addition, the results from this study could be also a result of microorganism activities. However, the influence of microbial activities on Fe plaque formation and persistence is still unresolved due to the complicated processes that control Fe mobility in natural soils and plants [11, 43-45].

4. CONCLUSION

This study is concentrated on the investigation of Fe plaque in the wetland plant (*Typha latifolia*, *Phragmites australis* and *Spartina alterniflora*) root epidermis. With the assistance of high-sensitivity and high resolution analytical apparatus and techniques provided by synchrotron X-ray microscope, this (sub)micro-scale investigation that Fe plaque is a cluster of Fe particles with a predominant species of ferric iron (i.e., Fe^{3+}). The synchrotron XRF mapping shows that

the distributions of Fe plaque in the wetland plant root cross-section is heterogeneous. Relatively high Fe concentrations are found in the root epidermis. As a result, this study has improved our current knowledge of Fe plaque concentration and distribution in the wetland plant root systems.

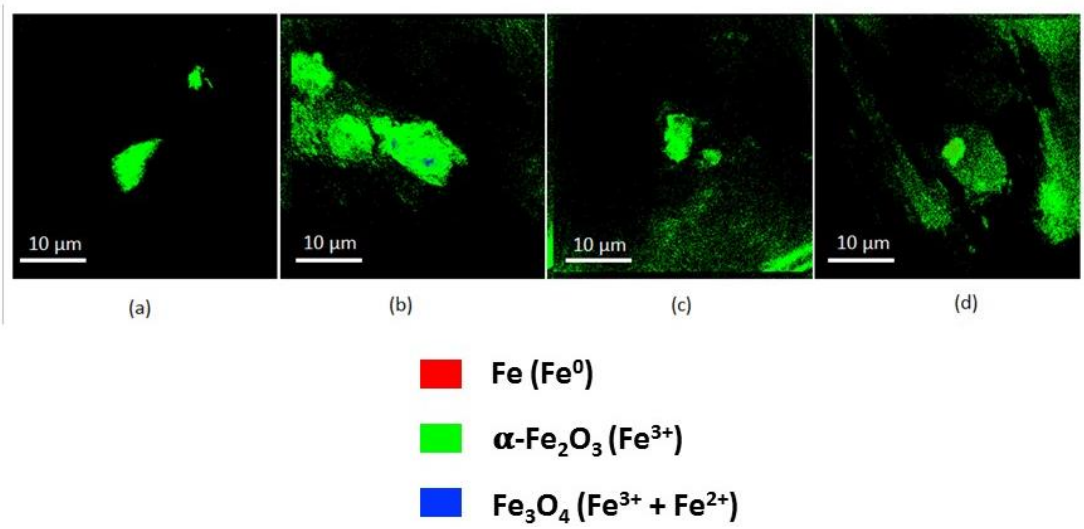

Figure 6 Synchrotron XANES measurement shows that Fe3+ is the major species in Fe plaque. The samples are (a) Spartina alterniflora collected in Chongming Island, Shanghai, in July 2013; (b) Phragmites australis collected in Chongming Island, Shanghai, in July 2013; (c) Phragmites australis collected in Liberty State Park, New Jersey, in May 2011; and (d) Spartina alterniflora collected in Chongming Island, Shanghai, in October 2006. The standard reference materials (Fe, α-Fe2O3 and Fe3O4) were used in the measurement. There is no Fe0 and Fe3O4 found during the measurement.

ACKNOWLEDGEMENTS

This work was supported in part by the State Key Laboratory of Estuarine and Coastal Research Open Research Fund (Ref #: SKLEC-KF201304 and SKLEC_KF201607) (HF, WZ, LY, WL), and the China Scholarship Council (YQ, HL). This project was also supported in part by the U.S. Department of Energy, Office of Science, Office of Workforce Development for Teachers, and Scientists (WDTS) under the Visiting Faculty Program (HF). Use of the NSLS was supported by the U.S. Department of Energy, Office of Science, Office of Basic Energy Sciences, under Contract No. DE-AC02-98CH10886. NSLS X27A was supported in part by the U.S. Department of Energy - Geosciences (DE-FG02-92ER14244 to The University of Chicago - CARS). This research used resources of the Advanced Photon Source, a U.S. Department of Energy (DOE) Office of Science User Facility operated for the DOE Office of Science by Argonne National Laboratory under Contract No. DE-AC02-06CH11357. Use of APS Beamline 8BM is partially supported by the National Synchrotron Light Source II, Brookhaven National Laboratory, under DOE Contract No. DE-SC0012704. The part of work in Biology Department, Brookhaven National Laboratory was supported in part by National Science Foundation through grant MCB-1051675 and by the Division of Chemical Sciences, Geosciences and Biosciences, Office of Basic Energy Sciences of the US Department of Energy through Grant DEAC0298CH10886 to C.J.L.

REFERENCES

1. W. Armstrong, Physiologia Plantarum **20** (4), 920-926 (1967).

2. R. E. Bacha and L. R. Hossner, Soil Science Society of America Journal **41** (5), 931-935 (1977).
3. C. Chen, J. Dixon and F. Turner, Soil Science Society of America Journal **44** (5), 1113-1119 (1980).
4. G. J. Taylor and A. A. Crowder, American Journal of Botany **70** (8), 1254-1257 (1983).
5. H. J. Liu, J. L. Zhang and F. S. Zhang, Environmental and Experimental Botany **59** (3), 314-320 (2007).
6. Q. Zhang, J. Liu, H. Lu, S. Zhao, W. Wang, J. Du and C. Yan, Environmental Nanotechnology, Monitoring & Management **4**, 6-11 (2015).
7. L. St-Cyr and P. G. C. Campbell, Biogeochemistry **33** (1), 45-76 (1996).
8. N. Rodríguez, N. Menéndez, J. Tornero, R. Amils and L. F. De, V., New Phytologist **165** (3), 781-789 (2005).
9. P. Pardha-Saradhi, G. Yamal, T. Peddisetty, P. Sharmila, J. Singh, R. Nagarajan and K. S. Rao, Biometals An International Journal on the Role of Metal Ions in Biology Biochemistry & Medicine **27** (1), 97-114 (2014).
10. V. Fuente, L. Rufo, B. H. Juárez, N. Menéndez, M. García-Hernández, E. Salas-Colera and A. Espinosa, Journal of Structural Biology **193** (1), 23–32 (2015).
11. T. Fresno, J. M. Peñalosa, J. Santner, M. Puschenreiter, T. Prohaska and E. Moreno-Jiménez, Environmental Pollution **216**, 215-222 (2016).
12. C. Liu, L. Wei, S. Zhang, X. Xu and F. Li, Rsc Advances **4** (100), 57227-57234 (2014).
13. W. J. Liu and Y. G. Zhu, Acta Ecologica Sinica **25** (2), 358-363 (2005).
14. W. J. Liu, S. P. Mcgrath and F. J. Zhao, Plant & Soil **376** (1-2), 423-431 (2013).
15. S. Greipsson and A. A. Crowder, Canadian Journal of Botany **70** (4), 824-830 (1992).
16. C. M. Hansel, M. J. La Force, S. Fendorf and S. Sutton, Environmental Science & Technology **36** (9), 1988-1994 (2002).
17. B. Sundby, C. Vale, Z. Caçador, F. Catarino, M. J. Madureira and M. Caetano, Limnology & Oceanography **43** (2), 245-252 (1998).
18. I. Koch and M. M. Nearing, J Environ Sci (China) **44**, 1-3 (2016).
19. Z. Ye, A. J. M. Baker, M. H. Wong and A. J. Willis, Aquatic Botany **61** (1), 55-67 (1998).

20. M. L. Otte, J. Rozema, L. Koster, M. S. Haarsma and R. A. Broekman, New Phytologist **111** (2), 309-317 (1989).
21. D. Lin and B. Xing, Environ Pollut **150** (2), 243-250 (2007).
22. H. Feng, Y. Qian, F. J. Gallagher, M. Wu, W. Zhang, L. Yu, Q. Zhu, K. Zhang, C.-J. Liu and R. Tappero, Environmental Science and Pollution Research **20** (6), 3743-3750 (2013).
23. H. Feng, W. Zhang, W. Liu, L. Yu, Y. Qian, J. Wang, J. J. Wang, C. Eng, C. J. Liu and K. W. Jones, Environmental Science & Pollution Research **22** (23), 18993-18994 (2015).
24. Y. Qian, H. Feng, F. J. Gallagher, Q. Zhu, M. Wu, C. J. Liu, K. W. Jones and R. V. Tappero, Journal of Synchrotron Radiation **22** (Pt 6), 1459-1468 (2015).
25. H. Feng, Y. Qian, F. J. Gallagher, W. Zhang, L. Yu, C. Liu, K. W. Jones and R. Tappero, Journal of Environmental Sciences **41**, 172-182 (2016).
26. T. Pardo, D. Martínez-Fernández, C. de la Fuente, R. Clemente, M. Komárek and M. P. Bernal, Environmental Pollution **219**, 296-304 (2016).
27. R. R. Martin, S. J. Naftel, W. Skinner, K. W. Jones and H. Feng, X-Ray Spectrometry **32** (5), 402-407 (2003).
28. R. R. Martin, S. J. Naftel, S. M. Macfie, K. W. Jones, H. Feng and C. Trembley, X-Ray Spectrometry **35** (35), 57-62 (2006).
29. J. Ablett, C. Kao, R. Reeder, Y. Tang and A. Lanzirotti, Nuclear Instruments and Methods in Physics Research Section A: Accelerators, Spectrometers, Detectors and Associated Equipment **562** (1), 487-494 (2006).
30. J. Wang, Y. c. Chen-Wiegart, Q. Yuan, A. Tkachuk, C. Erdonmez, B. Hornberger and M. Feser, Applied Physics Letters **100** (14), 143107 (2012).
31. J. Wang, Y. c. K. Chen-Wiegart and J. Wang, Nature communications **5** (2014).
32. J. Wang, Y. c. K. Chen-Wiegart and J. Wang, Angewandte Chemie **126** (17), 4549-4553 (2014).
33. J. Wang, Y. C. Chen-Wiegart and J. Wang, Chemical Communications **49** (58), 6480-6482 (2013).
34. C. M. Hansel, S. Fendorf, S. Sutton and M. Newville, Environmental Science & Technology **35** (19), 3863-3868 (2001).
35. N. K. Blute, D. J. Brabander, H. F. Hemond, S. R. Sutton, M. G. Newville and M. L. Rivers, Environmental Science & Technology **38** (22), 6074-6077 (2004).

36. I. A. Mendelssohn and M. T. Postek, American Journal of Botany **69** (6), 904-912 (1982).
37. G. J. Taylor and R. Rodden, American Journal of Botany **71** (5), 666-675 (1984).
38. T. Colmer, Plant, Cell & Environment **26** (1), 17-36 (2003).
39. X. Q. Mei, Y. Yang, N. F. Tam, Y. W. Wang and L. Li, Water research **50**, 147-159 (2014).
40. C. Wu, Z. Ye, H. Li, S. Wu, D. Deng, Y. Zhu and M. Wong, Journal of experimental botany **63** (8), 2961-2970 (2012).
41. X.-Q. Mei, Y. Yang, N. F.-Y. Tam, Y.-W. Wang and L. Li, Water research **50**, 147-159 (2014).
42. A. S. Templeton, J. D. Ostergren, T. P. Trainor, A. L. Foster, S. J. Traina, A. Spormann and G. E. B. Jr, Journal of Synchrotron Radiation **6** (3), 642-644 (1999).
43. M. A. Levan and S. J. Riha, Plant & Soil **95** (1), 33-42 (1986).
44. D. Emerson, J. V. Weiss and J. P. Megonigal, Applied & Environmental Microbiology **65** (6), 2758-2761 (1999).
45. J. V. Weiss, D. Emerson, S. M. Backer and J. P. Megonigal, Biogeochemistry **64** (1), 77-96 (2003).